THE ASTROPHYSICAL JOURNAL, 341:733–747, 1989 June 15

SIMULTANEOUS X-RAY, ULTRAVIOLET, AND OPTICAL OBSERVATIONS OF THE BL LACERTAE OBJECT PKS 2155−304

A. TREVES,[1] M. MORINI,[2] L. CHIAPPETTI,[3] A. FABIAN,[4] R. FALOMO,[5] D. MACCAGNI,[3] L. MARASCHI,[1] E. G. TANZI,[3] AND G. TAGLIAFERRI[6]

Received 1988 February 9; accepted 1988 October 24

ABSTRACT

X-ray observations of PKS 2155−304, performed at nine epochs in 1983–1985 with the *EXOSAT* satellite, are reported. The source was observed quasi-simultaneously in the far-UV with *IUE*, and in the optical and infrared with ESO telescopes. X-ray light curves with 400 s time resolution are derived. On two occasions the flux showed a rapid regular rising with a doubling time ~1 hr. Spectral fits performed on X-ray data averaged over each observation yield the following results. The medium energy data (1–10 keV) are well fitted by single power laws plus absorption, with energy index between 1.5 and 2. Marginal evidence for an absorption edge at ~7 keV is found in the best exposed spectrum. If we combine the ME data with those obtained with the low energy telescope (0.1–2 keV), evidence for some spectral depression at ~1 keV is found. This may be modeled with an edge at 660±26 eV with optical depth $\tau = 1.8 \pm 0.2$. The quasi-simultaneous ultraviolet and optical data allow the reconstruction of the energy distribution on several occasions. In all cases but one, the optical, UV, and X-ray intensities are correlated. However, the variability amplitudes decrease, and the time scales increase, with decreasing frequency. These results are indicative of a synchrotron origin for the X-rays and of distinct, but connected, emission regions for the X-ray, ultraviolet, and optical bands.

Subject headings: BL Lacertae objects — galaxies: individual (PKS 2155−304) — X-ray: sources — ultraviolet: spectra

I. INTRODUCTION

PKS 2155−304 is one of the brightest BL Lac objects at optical, UV, and X-ray frequencies. The X-ray source was discovered with the *HEAO 1* satellite (Schwartz *et al.* 1979; Griffiths *et al.* 1979) at a site where the *Ariel V* catalog reported confused emission (Cooke *et al.* 1978). The precise position obtained with the *HEAO 1* modulation collimator allowed the identification of the X-ray source with an optical counterpart with featureless spectrum and high polarization, thus revealing its BL Lac nature (Schwartz *et al.* 1979). The radio counterpart was recognized as the Parkes source 2155−304.

The redshift $z = 0.117$ was determined by Bowyer *et al.* (1984) from the detection of weak absorption lines in the faint nebulosity surrounding the source.

Since the first observations the source appeared variable in X-rays (e.g., Urry, Mushotzky, and Holt 1986 and references therein) as well as in the optical and UV (e.g., Maraschi *et al.* 1986).

Here we report on a series of observations of PKS 2155−304 obtained in 1983–1985 with the *EXOSAT* satellite in the 0.1–15 keV range, for a total of about 80 hr. For most of the X-ray observations simultaneous or quasi-simultaneous coverage in the UV (1200–3000 Å) was obtained with the *International Ultraviolet Explorer* (*IUE*). At a number of epochs optical spectrophotometry and infrared photometry were obtained at the telescopes of the European Southern Observatory (La Silla, Chile). Preliminary results on the X-ray data were presented in Morini *et al.* (1986, 1987).

The layout of the paper is as follows. The X-ray data are presented in § II. Spectral fits are given for various epochs, taking as a basic shape a power law with low-energy photoelectric absorption. The issues of an absorption feature at ~1 keV and at ~7 keV, and of a high-energy component are also discussed. The UV, optical, and infrared observations are described in § III. Correlations of variability in the various bands are presented in § IV. The spectral and variability data are discussed in the last section, in the context of present models for BL Lac objects.

II. X-RAY OBSERVATIONS

a) Observation Procedure and Background Subtraction

PKS 2155−304 was observed with the *EXOSAT* satellite at nine different epochs in 1983, 1984, and 1985 (see Table 1). The on-board instrumentation comprises three experiments (for reference see Taylor *et al.* 1981). The low energy (LE) experiment consists of a grazing incidence telescope, with a channel multiplier array (CMA) detector at the focal plane. Various filters can be interposed. The energy range of sensitivity is 0.05–2 keV. The medium energy (ME) experiment is an array of eight proportional counters each composed by an Ar + CO_2 filled cell and a Xe + CO_2 one. The detectors are grouped in two "halves" of the ME experiment, which can be independently offset to monitor the background. The energy range is 1–25 keV for the argon counters and 6–50 keV for the xenon ones. A gas scintillation proportional counter (GSPC), sensitive between 2–16 keV, was also available.

During all the 1983 and 1984 observations (see Table 1) the 3000 Å Lexan, aluminum-parylene, and boron filters were rotated in front of the CMA detector of the LE experiment, to

[1] Dipartimento di Fisica dell'Università, Milano, Italy.
[2] Istituto di Fisica Cosmica ed Applicazioni all'Informatica, C.N.R., Palermo, Italy.
[3] Istituto di Fisica Cosmica, C.N.R., Milano, Italy.
[4] Institute of Astronomy, Cambridge, England.
[5] Osservatorio Astrofisico, Padova, Italy.
[6] *EXOSAT* Observatory, Astrophysics Division, Space Sciences Department of ESA, ESTEC, The Netherlands.

TABLE 1

JOURNAL OF X-RAY OBSERVATIONS OF PKS 2155−304

UT time		Filter	LE counts per s	UT time		ME counts per s
1981 Oct 31	00:54–01:44.....	Lexan	0.755 ± 0.018	1983 Oct 31	00:25–14:56	2.03 ± 0.04
	02:54–04:47.....	Boron	0.038 ± 0.004			
	04:50–05:40.....	Lexan	0.743 ± 0.017			
	05:44–07:01.....	Al-Pa	0.227 ± 0.010			
	10:20–12:24.....	Boron	0.034 ± 0.004			
	12:37–13:38.....	Lexan	0.627 ± 0.014			
	14:08–16:02.....	Al-Pa	0.188 ± 0.006			
1983 Nov 29	18:47–19:03.....	Lexan	1.271 ± 0.083	1983 Nov 29	17:33–22–06	4.00 ± 0.09
	19:06–19:42.....	Al-Pa	0.422 ± 0.034			
	20:10–21:34.....	Boron	0.077 ± 0.006			
	21:45–22:05.....	Lexan	1.189 ± 0.048			
1984 Nov 6	13:52–14:25.....	Lexan	1.843 ± 0.035	1984 Nov 6	13:24–18:15	7.98 ± 0.05
	14:29–15:12.....	Al-Pa	0.644 ± 0.017			
	15:16–17:28.....	Boron	0.141 ± 0.005			
	17:37–18:08.....	Lexan	2.087 ± 0.050			
1984 Nov 7	09:58–10:30.....	Lexan	1.946 ± 0.041	1984 Nov 7	09:35–14:10	11.03 ± 0.05
	10:33–11:18.....	Al-Pa	0.712 ± 0.022			
	11:22–13:35.....	Boron	0.180 ± 0.006			
	13:39–14:11.....	Lexan	2.990 ± 0.008			
1984 Nov 11	11:43–12:04.....	Lexan	2.205 ± 0.096	1984 Nov 11	11:01–15:01	7.53 ± 0.07
	12:08–12:40.....	Al-Pa	0.784 ± 0.058			
	12:44–14:22.....	Boron	0.136 ± 0.006			
	14:26–15:03.....	Lexan	2.088 ± 0.041			
1985 Oct 24–25	11:00–01:18.....	Lexan	3.427 ± 0.010	1985 Oct 24–25	10:21–01:23	16.48 ± 0.05
1985 Nov 1	20:47–21:27.....	Lexan	1.668 ± 0.029	1985 Nov 1	20:24–22:37	4.88 ± 0.014
	21:31–22:34.....	Al-Pa	0.582 ± 0.014			
1985 Nov 2–3	08:18–01:15.....	Lexan	1.713 ± 0.007	1985 Nov 2–3	08:13–01:21	5.70 ± 0.03
1985 Nov 12–13	12:00–05:37.....	Lexan	1.240 ± 0.005	1985 Nov 12–13	11:24–05:37	3.02 ± 0.03

derive some spectral information in the LE band. The 1985 observations were instead performed using the 3000 Å Lexan filter (the most sensitive one) for the whole exposure, to obtain detailed light curves of the source in the soft X-ray band.

The LE count rates in the different filters were estimated from the images, integrating within a circle of 100″ of radius. The background was obtained from the surrounding annulus of 300″ external radius. Corrections for dead time were taken into account.

The ME observations were performed with the usual procedure of pointing half the counters at the source, and offsetting the other half to monitor the background. The details were, however, different for the various observations. Normally the offset ME counters are swapped at regular intervals during the observations, which allows the compensation of the different background spectra in the counters of the two ME halves (the background subtraction technique gives in this case source spectra corresponding to pairs of adjacent counters). The two short observations of 1983 November 29 and 1985 November 1 were, however, performed with the same half of the ME experiment pointing to the source during the whole observation: the background in the on-source counters was therefore estimated from that in the offset counters, corrected with data taken during the slew maneuvers before and after the source observation. In the observations of 1985 one detector was not usable, and source spectra from only three pairs of detectors were obtained. For a detailed description of the adopted procedure for background subtraction, we refer to Morini, Lipani, and Molteni (1987).

The background- and dead time-corrected LE and ME count rates are reported in Table 1. These are average values in the specified time intervals. The ME count rates refer to half the ME experiment; the observations of 1985 (when only three pairs of counters were available) were normalized to the previous ones multiplying by 4/3.

b) Light Curves

Light curves with integration times of 400 s are shown in Figure 1. The ME count rates correspond to the energy interval 1–6 keV, while the LE count rates refer to observations with the 3000 Å Lexan filter. Strong variability is apparent. In particular a variation of a factor 4 is found in 1984 November 6 and November 7, and a lesser flux increase (factor 2) in 1985 November 12. A detailed study of the variability on short time scales is in progress and will be reported elsewhere (Tagliaferri *et al.* 1988). The light curves of 1984 November 6, 7 have already been reported in Morini *et al.* (1986). The full dynamic range of variability in the LE and ME bands is 5, 10, respectively. The LE and ME intensities are clearly correlated, as illustrated in Figure 2 (see § IV).

c) Spectral Fits of the ME Data

In the background-subtracted argon spectra a net signal is apparent up to about 8 keV for lower states, and up to 15 keV for higher ones. Some signal is present in the xenon spectra only in the case of high-intensity states. The spectral fit of the data was performed with different models of increasing complexity. First we have fitted the ME argon data (over the 1–25 keV energy range) with a power law ($dN/dE = kE^{-\alpha}$), corrected for photoelectric absorption. The cross sections of Brown and Gould (1970), with corrections for Fe L and K shell effects, have been adopted. The data of each pair of counters—or each counter, depending on the background subtraction procedure (see above)—were fitted simultaneously according to the procedure of Morini, Lipani, and Molteni (1987). The

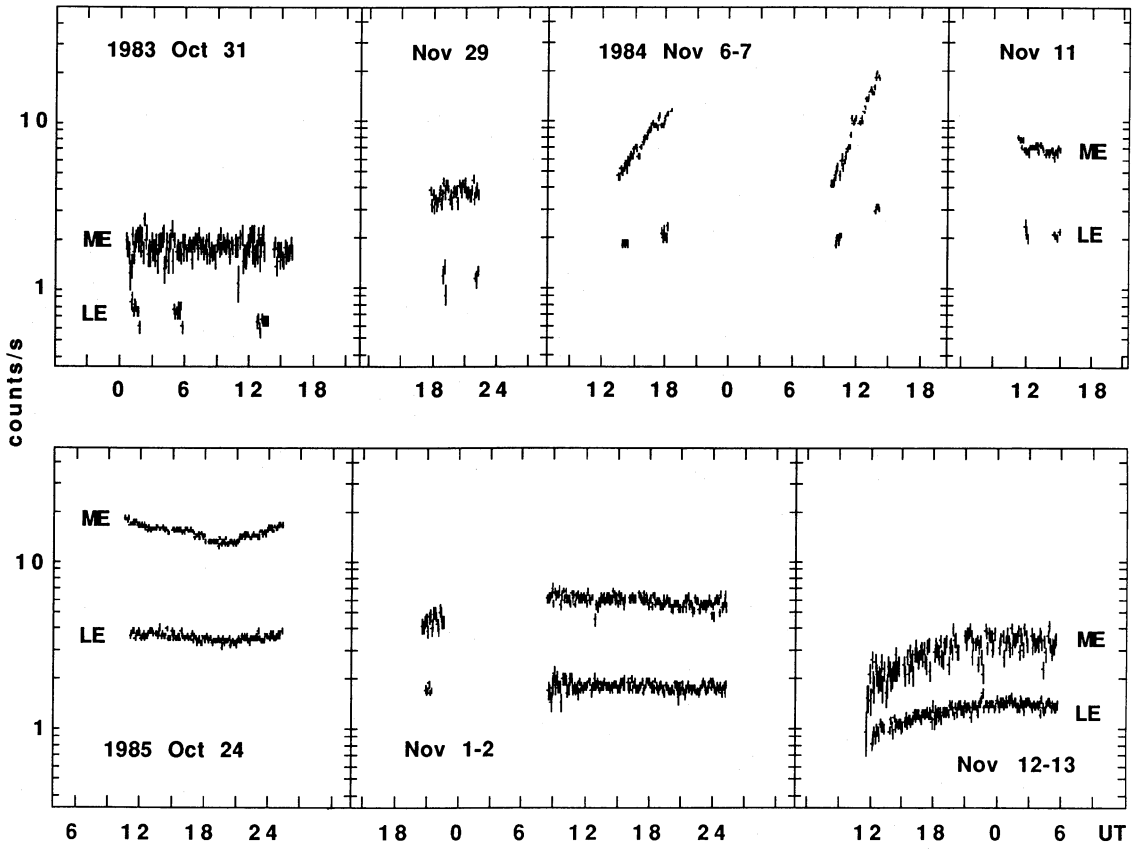

FIG. 1.—X-ray light curves of PKS 2155−304. *Upper traces:* ME count rates in the energy range 1–6 keV; *lower traces:* LE count rates with 3000 Å filter, effective energy range 0.2–0.6 keV.

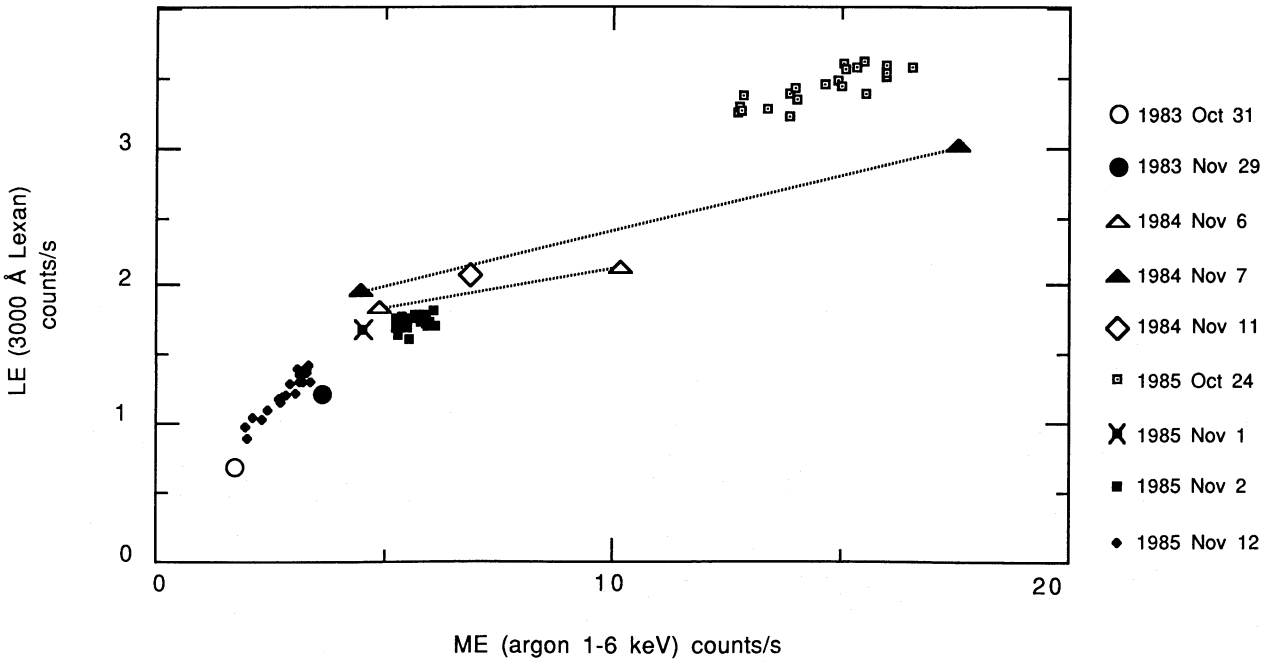

FIG. 2.—LE vs. ME count rates in temporal bins of 2400 s. The dotted lines connect two states of a same observation where flaring was observed.

normalizations of the relevant background components were included in the fits as additional free parameters. One pair of counters was excluded from the fit of the 1984 November 6 and November 7 data, because of a rather large deviation from the response of the other three pairs of detectors.

The best-fit values for the photon spectral index α and for the absorbing column density N_H are reported in Table 2A (the uncertainties in the parameters correspond to 1 σ, as determined from the diagonal terms of the inverse of the curvature matrix; see, e.g., Bevington 1969, p. 235). Some examples of pulse-height spectra are reported in Figure 3, together with the corresponding residuals. The observation of 1983 October 31, for which the fit is rather poor, corresponds to the lowest state of the source. The high χ^2 value for this observation is produced by contributions from all the pairs of counters, in particular at high energy, and can be attributed to background. The absorption column densities reported in Table 2 are of the order of 4×10^{21} cm^{-2}, significantly larger than expected from absorption in our Galaxy ($1.8 \pm 0.7 \times 10^{20}$ cm^{-2}, Stark *et al.* 1988).

In the best exposed spectra a signal is present in the xenon counters. In the region of overlap, the spectra obtained from these counters are consistent with those derived with the argon ones. In order to explore the existence of a high-energy tail, as suggested by some authors (see § V), we have summed the data corresponding to the six best exposed spectra. The result is shown in Figure 4, where the argon data are given in the energy range 1–10 keV, and the xenon data at higher energies. The 2 σ upper limit given in the figure corresponds to a flux of 3×10^{-5} photons cm^{-2} s^{-1} keV^{-1} in the energy band 12–50 keV, for a flat (photon index $\alpha = 0$), high-energy component.

i) *Search for an* Fe *Feature*

The 1985 October 24 observation, which represents the highest state of the source, and corresponds to a rather long observing time, is certainly best suited for a more detailed spectral study. The only feature which appears to be present is an absorption at 6–7 keV and is present in the data of each of the three pairs of counters. An enlargement of the reconstructed spectrum is shown in Figure 5, together with the residuals with respect to the power-law best fit. We have therefore fitted the data with an additional absorption edge, with optical depth of the form $\tau(E) = \tau o(E_o/E)^3$, with E_o in the range 3–8 keV. The values of the edge energy E_o and optical depth have been determined and are reported in Table 2B, in all cases but 1983 October 31 and 1985 November 2, when the inclusion of the absorption edge produces no significant reduction of the χ^2 value. The energy of the edge derived from the various observations is scattered and the mean value is 6.20 ± 0.27 keV, consistent with all the single values. In the last line of Table 2 we have assumed that the features were at 6.37 keV, corresponding to the cold Fe K absorption energy of 7.11 keV in the frame of the source, and give the corresponding optical depths. The only case in which the optical depth is statistically significant is 1985 October 24.

d) GSPC Spectra

We have also analyzed the spectra obtained with the GSPC, which may be valuable for spectroscopic studies, because of a better energy resolution. We found the GSPC spectra fully consistent with those presented above. However, due to the smaller effective area, the GSPC data for this relatively weak source do not improve the spectral results.

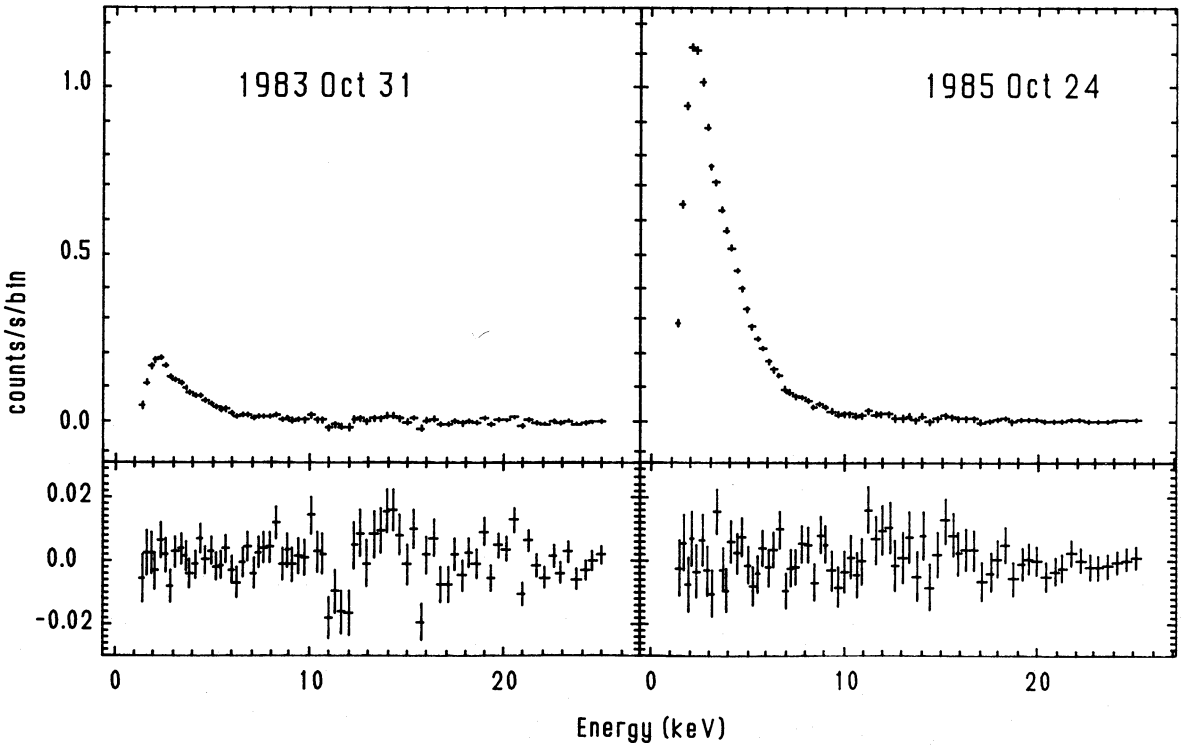

FIG. 3.—*Upper panels:* pulse height spectra for the sum of the ME argon counters in the 1–25 keV range for the 1983 Oct 31 (lowest state) and 1985 Oct 24 (highest state) data. *Lower panels:* residuals after fitting the data with a power-law spectrum and Fe K absorption with the parameters given in Table 2B. Note for the 1983 Oct 31 data the deviation from the fit in the energy range 10–20 keV, a region where there is no signal from the source. This is due to residuals fluorescent lines in the ME background, which are responsible for the high χ^2 values obtained fitting these data.

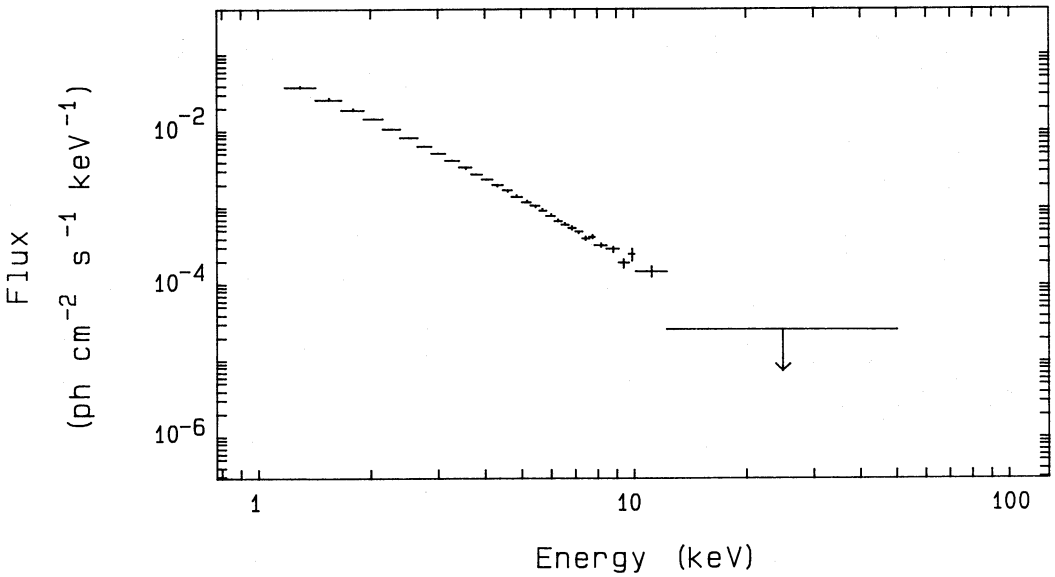

FIG. 4.—Deconvolved spectrum from the sum of six observations. Data are from the argon counters in the energy range 1–10 keV and from the xenon counters in the range 10–50 keV.

e) Spectral Fit of the Combined of ME + LE Data

The count rates in the different LE filters can be considered as independent energy channels, which can be combined with the ME channels. Here we have combined the spectra of all counters together into a single spectrum for each observation; the corresponding degrees of freedom are therefore decreased with respect to those considered in the previous section. For the observations when different filters have been used, we have interpolated the count rates for each filter to mid-observation.

The results of the LE + ME fits with an absorbed power law are given in Table 3C. It is apparent that the values of N_H are much smaller than those from the ME fits alone, and are consistent with the Galactic values. It is important to note that the reduced χ^2 values in most cases are large. This points toward a more complex spectral shape. The reconstructed spectra (Fig. 6), clearly indicate some deficiency in the keV region. This is the region between the ME and LE experiments, and the LE experiments yields only a spectral response corresponding to the filter interchange. Our data therefore are not capable of yielding a direct indication of the spectral shape at ~1 keV, but can be used to test the goodness of a given spectral shape. The values of the corresponding parameters will then be determined with an accuracy depending on the source statistics.

A first possibility is to consider a two power-law spectrum (plus absorption), to accounting for the entire LE + ME range. In fact Barr *et al.* (1988) in a global study of BL Lac objects observed with *EXOSAT* showed that the spectra are significantly better fitted with broken steepening power laws than by a single power. Our fits (Table 3B), which consider only the cases where count rates in all three LE filters are available, indicate only a little improvement. Note that the fitting procedure leads to a steeper spectrum at lower energies and that the break energy E_{int} turns out to be in the region covered by the LE experiment, where the resolution is poor.

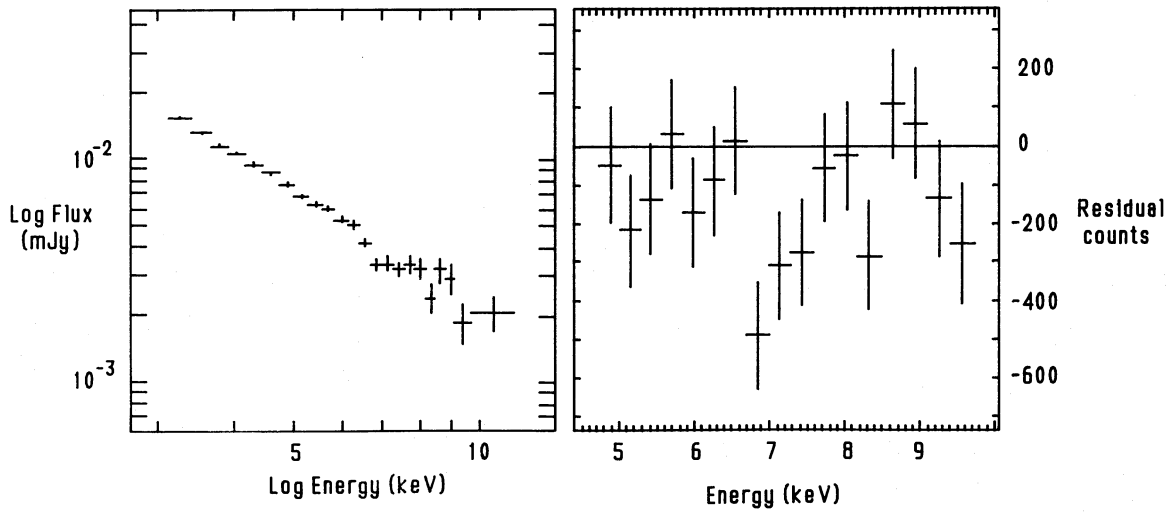

FIG. 5.—*Left panel:* detail of the spectrum of PKS 2155−304 of 1985 Oct 24 deconvolved with a power law, showing a possible absorption feature at 6–7 keV. *Right panel:* residuals with respect to a power law.

TABLE 2

SPECTRAL FIT OF THE ME DATA

Parameter	1983 Oct 31	1983 Nov 29	1984 Nov 6	1984 Nov 7	1984 Nov 11	1985 Oct 24	1985 Nov 1	1985 Nov 2	1985 Nov 12
A. Power Law									
α_{ph}	2.78 ± 0.15	2.90 ± 0.22	2.58 ± 0.7	2.68 ± 0.06	3.02 ± 0.08	2.76 ± 0.03	2.98 ± 0.29	2.78 ± 0.06	2.91 ± 0.1
$N_H(10^{20}$ cm$^{-2})$	35 ± 29	74 ± 43	42 ± 14	56 ± 11	72 ± 15	38 ± 6	46 ± 51	27 ± 10	23 ± 17
χ^2	475.4	283.2	208.6	221.3	342.9	243.1	150.1	198.0	233.8
d.o.f.	286	291	206	206	278	203	134	203	203
B. Power Law + Iron *K* Absorption									
α_{ph}	2.69 ± 0.18	2.74 ± 0.23	2.55 ± 0.1	2.62 ± 0.06	3.01 ± 0.08	2.73 ± 0.03	2.98 ± 0.29	2.77 ± 0.06	2.92 ± 0.1
$N_H(10^{20}$ cm$^{-2})$	12 ± 29	45 ± 44	38 ± 15	45 ± 12	70 ± 12	27 ± 6	47 ± 51	26 ± 10	24 ± 18
E_0(keV)	...	5.75 ± 0.92	6.48 ± 1.22	5.68 ± 0.77	6.95 ± 1.12	6.34 ± 0.41	7.49 ± 0.63	...	6.79 ± 1.17
τ_0	...	0.75 ± 0.72	0.15 ± 0.16	0.14 ± 0.10	0.21 ± 0.27	0.23 ± 0.09	−0.88 ± 0.89	...	0.36 ± 0.50
χ^2	475.8	279.8	207.0	215.5	342 ± .3	228.8	149.1	198.0	232.0
d.o.f.	284	289	204	204	276	201	132	201	201
$\tau_0(E_0 = 6.37$ keV)[a]	−0.16 ± 0.30	0.85 ± 0.83	0.14 ± 0.13	0.12 ± 0.1	0.20 ± 0.21	0.24 ± 0.07	−0.53 ± 0.49	0.00 ± 0.12	0.26 ± 0.27

[a] Optical depth fixing the energy of the iron absorption at 6.37 keV.

TABLE 3

SPECTRAL FIT OF THE ME + LE DATA

Parameter	1983 Oct 31	1983 Nov 29	1984 Nov 6	1984 Nov 7	1984 Nov 11	1985 Oct 24	1985 Nov 1	1985 Nov 2	1985 Nov 12
A. Single Power-Law Model, LE + ME Data									
α_{ph}	2.70 ± 0.31	2.67 ± 0.48	2.44 ± 0.020	2.46 ± 0.014	2.73 ± 0.022	2.63 ± 0.01	2.75 ± 0.04	2.67 ± 0.015	2.82 ± 0.03
$N_H(10^{20}$ cm$^{-2})$	1.47 ± 0.12	1.78 ± 0.22	1.21 ± 0.06	1.46 ± 0.06	2.11 ± 0.11	2.38 ± 0.05	1.81 ± 0.17	1.74 ± 0.07	1.87 ± 0.12
χ^2	157.44	95.75	110.79	133.98	194.55	119.02	64.2	78.51	72.38
d.o.f.	74	75	72	72	72	68	69	68	68
ϕ(0.1–2 keV)[a]	0.87	1.81	2.9	3.7	3.65	6.64	2.27	2.63	1.8
ϕ(2–10 keV)[a]	0.083	0.19	0.54	0.66	0.33	0.76	0.19	0.27	0.13
L(0.1–10 keV)[b]	1.41	2.98	5.07	6.43	5.85	10.88	3.82	4.27	2.83
B. Broken Power-Law Model, LE + ME Data									
α_1	5.44 ± 1.6	4.46 ± 1.52	3.20 ± 0.53	14.0 ± 1.5	6.67 ± 1.13				
α_2	2.65 ± 0.05	2.62 ± 0.07	2.42 ± 0.02	2.50 ± 0.02	2.75 ± 0.03				
E_{int}(keV)	0.43 ± 0.07	0.48 ± 0.16	0.56 ± 0.20	0.31 ± 0.01	0.47 ± 0.07				
$N_H(10^{20}$ cm$^{-2})$	3.51 ± 1.43	3.23 ± 1.28	1.90 ± 0.43	6.62 ± 1.41	6.23 ± 1.38				
χ^2	134.13	82.91	94.74	101.49	107.8				
d.o.f.	72	73	70	70	70				
C. Power Law + Absorption Edge									
α_{ph}	2.79 ± 0.04	2.75 ± 0.06	2.52 ± 0.02	2.52 ± 0.02	2.92 ± 0.04	2.74 ± 0.02	2.94 ± 0.17	2.76 ± 0.03	2.89 ± 0.05
$N_H(10^{20}$ cm$^{-2})$	1.81 ± 0.17	2.12 ± 0.34	1.52 ± 0.11	1.60 ± 0.09	3.11 ± 0.31	2.90 ± 0.11	2.56 ± 0.85	2.12 ± 0.16	2.15 ± 0.22
E_{ox}(keV)	0.61 ± 0.07	0.78 ± 0.12	0.83 ± 0.10	0.57 ± 0.05	0.717 ± 0.04	0.66	0.524 ± 0.1	0.66	0.66
τ_{ox}	3.1 ± 1.2	1.8 ± 0.6	1.1 ± 0.30	1.8 ± 0.4	2.9 ± 0.4	1.9 ± 0.4	5.0 ± 7.7	1.8 ± 0.5	1.2 ± 0.8
χ^2	133.76	79.79	77.26	95.55	77.26	71.62	62.64	65.81	69.75
d.o.f.	72	73	70	70	70	67	67	67	67
					5.85	10.88	3.82	4.27	2.83

[a] 10^{-10} ergs cm^{-2} s^{-1}.
[b] 10^{45} ergs s^{-1}

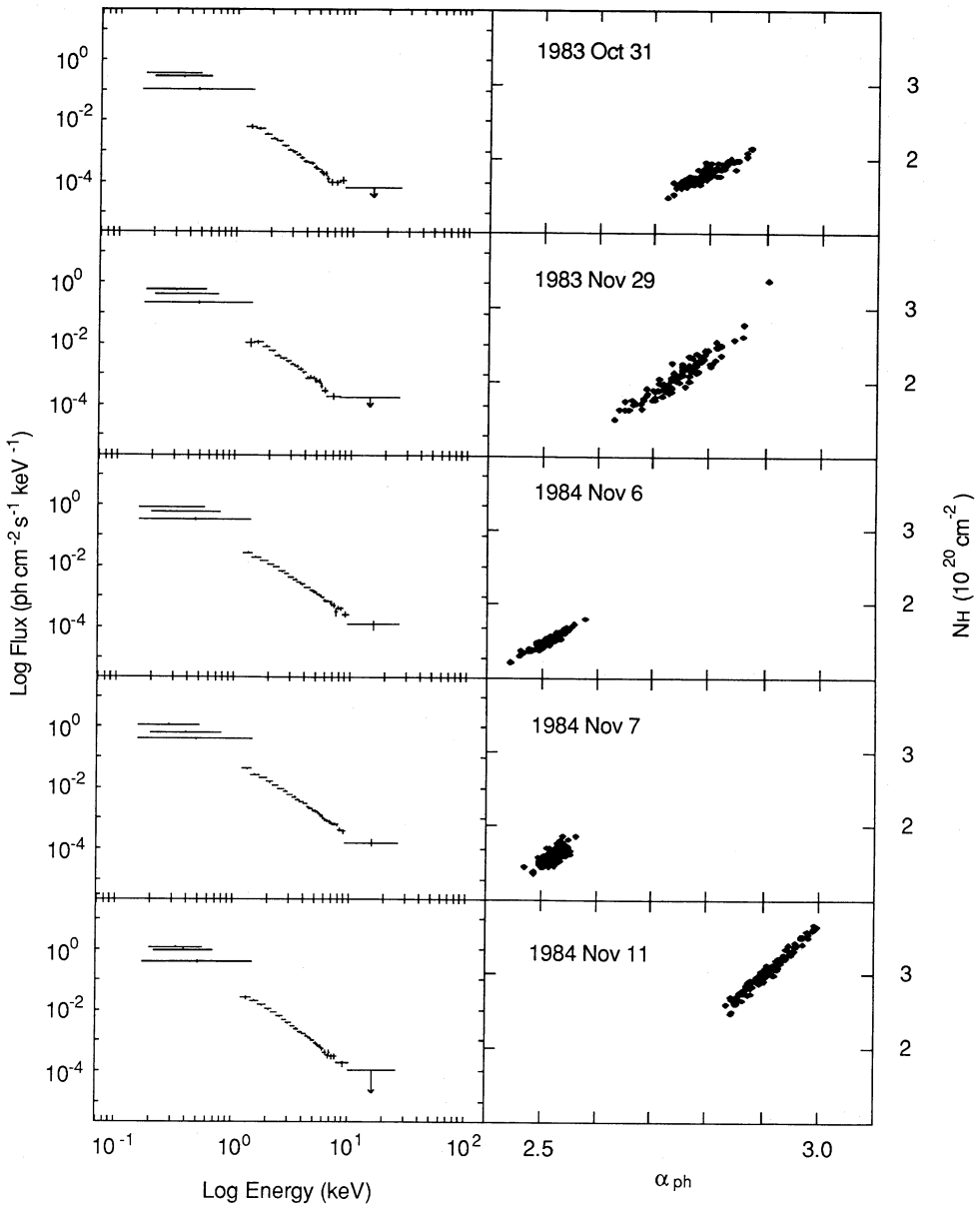

FIG. 6a

FIG. 6.—Deconvolved spectra of PKS 2155−304 at various epochs (*left panels*). The horizontal bars for the LE data correspond to the energy ranges of sensitivity for the various LE filters (80% of the photon flux for the assumed incident spectrum convolved the detector response, therefore these ranges are different at the different epochs). The α-N_H confidence intervals (*right panels*) are determined with a bootstrap sampling technique.

We are therefore led to consider that besides the interstellar absorption, some additional absorption occurring at $\sim$1 keV may be present, as suggested by the reconstructed spectra. The situation appears similar to that of other extragalactic sources, where medium-energy absorption and excess low-energy flux suggest the presence of a partially ionized absorbing medium (see, e.g., Halpern 1984). In particular for the case of PKS 2155−304 the results of Canizares and Kruper (1984) show the presence of a deep absorption trough at 0.6–0.7 keV. A complex photoionization model should be used to properly fit the data. In our case, however, the lack of energy resolution in the LE data suggests a simpler analysis. At the relevant temperatures ($T \sim 10^6$–10^7 K) the absorption in the 0.1–1 keV range is mainly from partially ionized oxygen and can be roughly approximated by a single photoelectric edge (see, e.g., the figures in Krolik and Kallman 1984). We have therefore added to the power-law model an absorption edge with energy (<1 keV) and absorption depth as free parameters. Two of the fitted parameters (the Galactic absorption N_H and the absorption edge energy) depend now on the LE data, and a fit can be performed for all observations except 1985 October 24 and November 2 and 12, when only one filter was used. The results of the new fits are given in Table 3B. The χ^2 values have significantly decreased, as confirmed by F test (the chance probability for a similar reduction is less than 10^{-14} in the case of 1984 November 11). The average value of the energy of the edge is $\langle E_{ox} \rangle = 660 \pm 26$ eV, and the average optical depth $\tau_{ox} = 1.8 \pm 0.2$. In Table 3B we have also reported the results

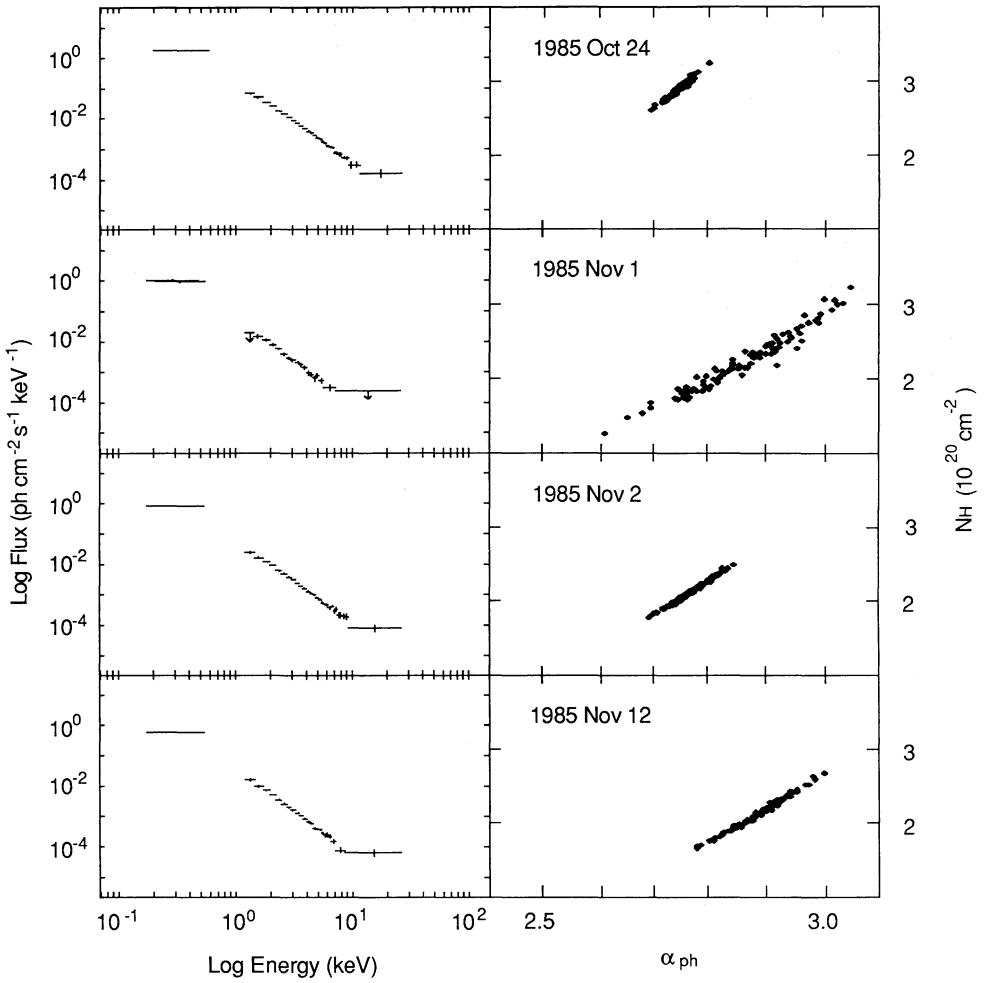

FIG. 6*b*

of the fit for the 1985 October 24 and November 2 and 12 data, for which the value of E_{ox} was fixed at 660 eV.

The absorption edge was therefore included in the absorbed power law in reconstructing the spectra in the entire LE + ME range. These are reported in Figures 6*a–j*. The confidence intervals in α-N_H shown in Figure 6 were determined by bootstrap sampling of the data (e.g., Simpson and Mayer-Hasselwander 1986). Since 100 points are reported, their envelope corresponds to ~99% confidence contours. In Figure 7 the spectrum of 1984 November 11 has been magnified and the best fit has been superposed in order to show clearly the contribution of the absorption edge. The last line of Table 3 gives the observed luminosities derived from the best-fit models in the 0.1–15 keV range (for $z = 0.117$ and $H_0 = 100$ km s^{-1} Mpc^{-1}), and assuming isotropic emission.

III. UV, OPTICAL, AND INFRARED OBSERVATIONS

a) Ultraviolet Observations

PKS 2155−304 was observed in the far-UV band (1200–3000 Å) with the *International Ultraviolet Explorer* in correspondence with all the X-ray *EXOSAT* observations, but for 1985 November 1–2. A list of the UV observations is detailed in Table 4. All the spectra were treated as specified in Maraschi *et al.* (1986), where some of them were already presented. For each spectrum average fluxes in consecutive bins of 50 Å were determined, avoiding flaws of the cameras, hot pixels, and reseau marks. Short wavelength (1200–1950) and long wavelengths (2000–3000) exposures obtained in close succession were combined and a power law $F_\lambda \propto \lambda^{-\alpha}$ was fitted to the data using a χ^2 minimization procedure. No reddening correction was introduced, consistent with the absence of an absorption feature at 2200 Å and with the hydrogen column deduced from radio and X-ray data (see § II). Intensity and slopes for the various spectra are given in Table 4. Slopes refer to the fit of the continuum in the 1200–3000 Å range. They agree with those obtained by Urry *et al.* (1988), who used a more refined procedure of data analysis.

IUE spectra of PKS 2155−304 from 1979 to 1986 have been studied by Maraschi *et al.* (1986), and Urry *et al.* (1988). The observations reported here cover essentially the entire range of the observed UV variability (a factor of 2), the 1985 November 12 state being the lowest ever observed and that of 1984 November 7, among the highest.

b) Fine Error Sensor Data

In correspondence of each UV exposure (but LWR 2330) the source was monitored with the fine error sensor onboard the *IUE* satellite. The detector has a broad spectral response in the 4000–8000 Å band. In Table 4 the FES count rates are given,

TABLE 4

JOURNAL OF *IUE* OBSERVATIONS

DATE	SPECTRAL IDENTIFICATION	EXPOSURE (s)	ergs cm^2 s Å (1500)	ergs cm^2 s Å (2500)	α_λ	FES	V
1983 Oct 31	SWP 21418	60	7.8			60	13.5
					0.95 ± 0.02		
1983 Oct 31	LWP 2189	34		4.4		58	13.6
1983 Nov 29	SWP 21637	120	9.3			82	13.2
					1.0 ± 0.02		
1983 Nov 29	LWP 2330	60		5.6			
1984 Nov 6	SWP 24406	105	13.1			96	13.0
					1.1 ± 0.02		
1984 Nov 6	LWP 4738	70		7.2		100	13.0
1984 Nov 7	SWP 24410	70	14.5			108	12.9
					1.12 ± 0.02		
1984 Nov 7	LWP 4746	37		8.2		108	12.9
1984 Nov 11	SWP 24445	100	12.9			109	12.9
					1.06 ± 0.02		
1984 Nov 11	LWP 4782	40		7.1		109	12.9
1984 Nov 11	LWP 4783	20		6.9		109	12.9
1985 Oct 24	SWP 26974	90	10.6			64	13.5
					1.24 ± 0.02		
1985 Oct 24	LWP 6986	40		5.2			
1985 Nov 12	SWP 27094	90	7.0			53	13.7
					1.05 ± 0.02		
1985 Nov 12	LWP 7082	39	3.3	3.3		53	13.7

together with the corresponding V magnitudes (Holm and Crabb 1979). A fixed value of $B-V = 0.47$ was adopted. The uncertainty on the magnitudes is ~ 0.1.

c) Ground-Based Optical and Infrared Observations

Optical observations were obtained with the 1.52 m ESO telescope (Boller and Chivens spectrograph + image dissector scanner) at a dispersion of 224 Å per mm. Epochs and spectral range are detailed in Table 5. No strict simultaneity to *IUE* observations could be achieved, typical time differences being however restricted to less than one day. Allowing for a typical interday variability of ~ 0.1 mag, as derived from extensive optical monitoring, a general agreement between FES and ground-based data is found.

Infrared observations with the 3.6 m ESO telescope equipped with a InSb photometer were obtained in the photometric bands J ($\lambda = 1.25$ μm), H ($\lambda = 1.65$ μm), and K ($\lambda = 2.2$ μm). Magnitudes and fluxes, as derived in the photometric system in use at ESO, are reported in Table 5. Some results on these observations were published in a preliminary form in Tanzi *et al.* (1984) and Maraschi *et al.* (1986).

The intensity in the optical varies by a factor of 2, with $12.8 < m_v < 13.7$, a range similar to that covered by the 1978–1981 photometry of Miller and McAlister (1983). No color

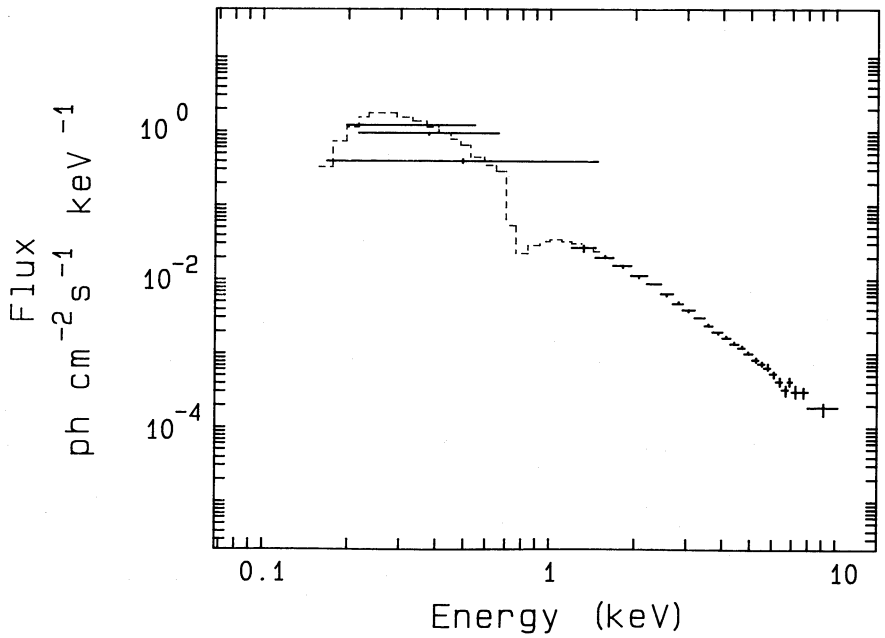

FIG. 7.—The deconvolved spectrum and best-fit model (*dashed histogram*) for 1984 Nov 11

TABLE 5

OPTICAL AND INFRARED OBSERVATIONS

Date	Instrument	Range/magnitude	Flux × 10^{15} ergs cm^{-2} s^{-1} Å^{-1}
1983 Aug 16 to 18	Photometer	$J = 11.84$	6.0
		$H = 11.22$	4.1
		$K = 10.60$	2.4
		$L = 9.2$	1.1
1983 Oct 29	IDS	4000–8000Å	
		$V = 13.2$	19
1983 Oct 30	IDS	4000–8000Å	
		$V = 13.4$	16
1983 Nov 20	IDS	4000–8000 Å	
		$V = 13.1$	21
1983 Nov 30	Photometer	$U = 12.67$	36
		$B = 13.37$	30
		$V = 13.1$	21
1983 Dec 1	Photometer	$U = 12.6$	38
		$B = 13.4$	29
		$V = 13.2$	19
		$R = 12.9$	16
		$I = 12.5$	12
1983 Dec 2	Photometer	$U = 12.68$	35
		$B = 13.42$	28
		$V = 13.13$	20
		$R = 12.87$	16
		$I = 12.38$	13
1983 Dec 4	Photometer	$U = 12.63$	37
		$B = 13.37$	30
		$V = 13.12$	20
		$R = 12.82$	17
		$I = 12.37$	14
1984 Sept 6 to 7	Photometer	$J = 11.53$	7.9
		$H = 10.91$	5.4
		$K = 10.22$	3.4
		$L = 8.9$	1.4
1984 Nov 8	IDS	4000–8000 Å	
		$V = 12.8$	27
1984 Nov 9	IDS	4000–8000 Å	
		$V = 12.8$	27
	Photometer	$J = 11.47$	8.4
		$H = 10.82$	5.9
		$K = 10.19$	3.5
		$L = 8.6$	1.9
1984 Nov 10	IDS	4000–8000 Å	
		$V = 12.9$	25
1984 Nov 11	IDS	4000–8000 Å	
		$V = 12.9$	25
		$J = 11.52$	8.0
		$H = 10.87$	5.7
		$K = 10.21$	3.5
1984 Nov 12	IDS	4000–8000 Å	
		$V = 12.9$	25

intensity correlation can be found in our data. Comparing the spectra of 1983 October 29, corresponding to a low state, with that of 1984 November which is a high state, it is found that the higher state is harder ($\alpha_v = 0.45$; $B-V = 0.47$) than the lower one ($\alpha_v = 0.7$; $B-V = 0.3$). This is just the opposite of the tendency found by Miller and McAlister (1983) in their data.

IV. CORRELATIONS BETWEEN THE VARIOUS SPECTRAL BANDS

a) Correlations between Intensities

A plot of the LE Lexan count rates versus the simultaneous ME count rates is given in Figure 2. The observations at the different epochs are represented by different symbols. Each point corresponds to a temporal bin of 400 s. It is apparent that the fluxes in the two bands are strongly correlated and, in fact, considering the entire set of observation with the mean fluxes reported in Table 1, we find that the chance probability P for the correlation is $P < 6 \times 10^{-5}$ (see Table 6). The slope of the correlation seems to depend on the state of source. At low intensity the ratio R of the LE counts to the ME counts is clearly higher than at higher intensities. It is noticeable that during the two epochs when a flare was observed (1984 November 6 and 7), the reduction of R with intensity is substantial, clearly indicating a hardening of the source. Leads or lags between the different X-ray bands are not apparent from the light curves. A careful cross correlation analysis is under way (see Tagliaferri *et al.* 1988).

Strong correlation is found also between the UV and optical fluxes as given by the FES. The typical differences between mid-observations in the two bands are ~1 hr. The situation is more complex when one correlates the optical-UV with the X-rays. Here typical distances between mid-observations may

TABLE 6

PROBABILITY OF CORRELATION BETWEEN VARIOUS SPECTRAL PARAMETERS

A. Correlation between Intensities

Parameter	F_{1500}	F_{LE}	F_{ME}
F_{opt}	0.9838–0.9903[a]	0.234–0.364	0.540–0.565
$F_{1500\,Å}$	...	0.686–0.764	0.883–0.897
F_{LE}	...	...	0.999939–0.999999

B. Correlation between Spectral Parameters

Parameter	N_H	α_{UV}	α_X	E_{ox}	τ_{ox}
F_{opt}	0.–0.577	0.0731	0.506–0.975	0.–1.	0.123–0.279
$F_{1500\,Å}$	0.354–0.580	0.278–0.929	0.486–0.989	0.–1.	0.–0.483
F_{LE}	0.876–0.936	0.986–0.998	0.433–0.506	0.–1.	0.–0.718
F_{ME}	0.638–0.727	0.919–1.	0.353–0.500	0.–1.	0.–0.275
N_H		0.190–0.988	0.805–1.	0.–1.	0.617–0.957
α_{UV}			0.002–0.510	0.–1.	0.–1.
α_X				0.–1.	0.–1.
E_{ox}					0.–1.

[a] 90% confidence intervals for the probability of correlation.

be of several hours. The ME and LE fluxes do not correlate significantly with the UV flux ($P \sim 15\%$, $P > 30\%$). The optical-UV to X-ray correlations are made poor by the observations of 1985 October 24, when the X-ray flux in both bands is very high, while the optical and UV are at a low level.

b) *Correlation between Spectral Parameters*

It is clear from Table 3 that there is strong evidence for spectral variability. The chance probability of a constant α and N_H is $P < 10^{-6}$ and, $P \approx 5\%$ for E_{ox} and τ, respectively. Therefore it is of interest to search for correlations between the spectral parameters and the intensities in the various bands. The only significant correlation is found between the UV slope and the X-ray intensities. For the LE X-ray intensity the correlation has a confidence level larger than 98%, in the sense that the harder the UV spectrum, the higher the X-ray intensity. A similar correlation is found between the UV slope and the ME intensity (see Fig. 8). Note that F_{UV} does not seem to correlate with α_{UV}, a point which was already noticed (Maraschi *et al.* 1986 and Urry *et al.* 1988). A correlation of the X-ray slope with the optical-UV flux is not excluded by our data, in the sense that the higher the optical-UV intensity, the flatter the X-ray spectrum. The correlation is better ($P > 90\%$) if the 1984 November 11 data, when the X-ray spectrum was very steep and the optical UV in a high state, are excluded.

V. DISCUSSION

a) *Comparison with Previous Observations*

Since its discovery in 1977 PKS 2155−304 was observed numerous times in X-ray, with different satellites. The fluxes measured with various experiments onboard *HEAO 1* and the *Einstein Observatory* from 1977 to 1980 are summarized in Table 8 of Urry *et al.* (1986) (see also Snyder *et al.* 1980 and Agrawal *et al.* 1987). The fluxes at 2 keV, averaged over each observation epoch range from 3×10^{-3} to 2×10^{-2} photons per cm^2 s keV. Rapid variability has been detected on several

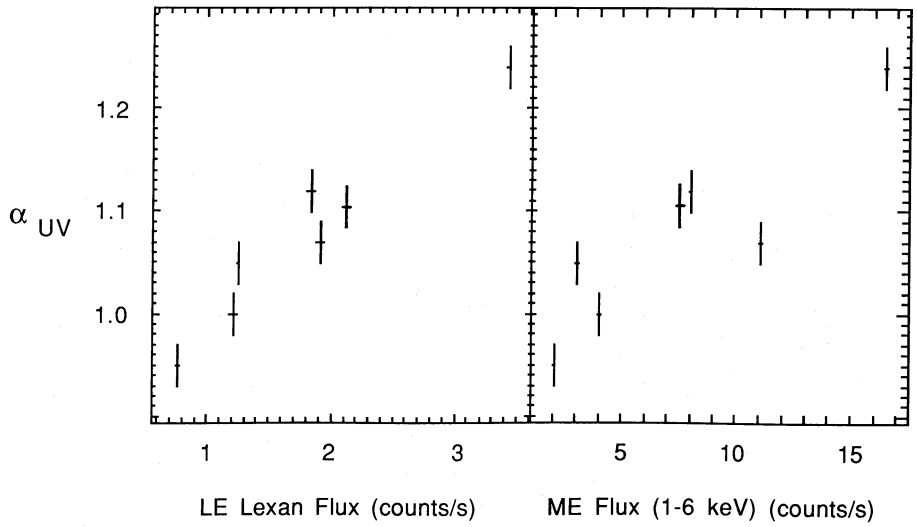

FIG. 8.—Spectral index α_λ in the UV band vs. X-ray intensity. *Left frame:* LE count rates; *right frame:* ME count rates.

occasions, particularly significant is the fading of the source from 3.5×10^{-2} to 10^{-2} photons per cm^2 s keV in 36 hr observed in 1977 November (Urry and Mushotzky 1982). In 1983 October 1–3, about a month before our first *EXOSAT* observation, the source was observed with *TENMA* at an average state (7 to 13 10^{-3} photons per cm^2 s keV; Miyoshi *et al.* 1986). Our observations, ranging from 4 to 43×10^{-3} photons per cm^2 s keV, cover essentially all the intensity states observed before. The observation at the end of 1984 November 7 shows the highest state ever detected.

Comparison with previous observations regarding the spectral shape is more complex, since the various instruments cover different energy ranges. A fit of the *Einstein* SSS data (0.5–4.5 keV, Urry *et al.* 1986) with a power law gives slopes close to ours. The hydrogen column density is much larger than that found by us combining the LE and ME X-ray data, which, as noted above, agrees well the Galactic value. The difference is most probably due to the fact that the low bound of the *EXOSAT* energy range is at lower energies. In fact the values of N_H of Urry *et al.* (1986) are close to those we obtain with the ME experiment alone.

The deficiency of flux at 600 eV, discussed in the previous section, is close to that reported by Canizares and Kruper (1984). These authors, in a long observation with the objective grating spectrometer onboard the *Einstein Observatory*, found an absorption feature, which could be fitted either by a wide absorption or by an edge ($E_{ox} = 590 \pm 20$ eV, $\tau_{ox} = 2.1^{+1}_{-0.8}$). Assuming that the continuum is described by a single power law, our results seem to favor the latter interpretation. In the *Einstein* SSS data the edge interpretation seems acceptable only if $E_0 < 500$ eV. We note that the favoring of the edge interpretation, and the disagreement with the SSS data may be removed, if a more complex continuum is chosen, e.g., with a steeper power law at lower energies. For this reason we do not enter into the discussion of the origin of the edge, and the related difficulties for its interpretation (see, e.g., Canizares and Kruper 1984).

The absorption feature at ~ 7 keV for which we found marginal evidence in one of our observations was never reported before in this source, but is expected in models which account for the 600 eV feature (see Krolik *et al.* 1985).

Urry and Mushotsky (1982) and Urry *et al.* (1986) have found a hard spectral component in both *HEAO 1* A2 data and in the MPC of the *Einstein Observatory*, dominating above ~ 10 keV. The *HEAO 1* A4 results (Bezler, Gruber, and Rothschild 1988) indicate that the flat component, if present, does not extend above 70 keV. No indication of a high-energy tail is found in our data with a 2 σ upper limit close to the detection level of Urry and Mushotzky (1986) (see § IIc). In view of the large variability of the source, one can still reasonably assume that the appearance of the tail is a sporadic phenomenon.

b) *The Broad-Band Energy Distribution and Variability*

An important result of our observations is the detection of large variability of the source in all examined spectral bands. A comparison of the light curves in optical, UV (2500 Å and 1500 Å), low-energy X-rays ($E \approx 0.2$ keV) and medium-energy X-rays ($E \approx 3$ keV) is given in Figure 9. Even if the coverage in the various bands is far from uniform, the figure suggests an increase of the source variability with increasing energy. In fact define the variability dynamic range

$$d = F_{max}/F_{min} \qquad (1)$$

and the variability time scale

$$t_D = F(\Delta F/\Delta t)^{-1} . \qquad (2)$$

In the optical and UV $d \approx 2$, in soft X-rays $d \approx 5$, in medium-energy X-rays $d \sim 10$. The minimum values of t_D in the various bands are

$$t_D(\text{opt}) \approx 90 \text{ days} ; \quad t_D(1500 \text{ Å}) \approx 50 \text{ days} ;$$
$$t_D(0.2 \text{ keV}) \approx 7 \text{ hr} ; \quad t_D(3 \text{ keV}) \approx 2 \times 10^3 \text{ s} . \qquad (3)$$

The optical and UV time scales have been deduced from the values reported in Tables 4 and 5. The procedure for calculating the minimum time scale in the X-rays which corresponds to variability within a single observation (1984 November 7) has been described in Morini *et al.* (1986). A decrease of the variability properties with increasing wavelength is consistent with the absence of variability on time scales of years in the radio band (Ulvestad and Antonucci 1986). Note that an increase of variability with energy appears to be a general property of blazars (Impey and Neugebauer 1988). For PKS 2155−304 the property extends to medium-energy X-rays, a region unexplored for most blazars.

The overall spectrum of PKS 2155−30 from infrared to X-ray frequencies is reported in Figure 10, for two epochs (1983 October 31, 1984 November 11), when the source was in a low and in a high state, respectively. The time differences between mid observations in optical, UV, and X-rays at each epoch are less than a day. A steepening of the spectrum from the infrared to the UV is apparent with $\Delta\alpha = 0.35$ (0.5), between the optical and UV for the lower (higher) state. A further steepening by $\Delta\alpha \approx 1$ is found comparing the UV with the X-rays.

The overall energy distribution of BL Lac objects is commonly interpreted in terms of the so-called synchrotron self-Compton (SSC) model. An application of the model to PKS 2155−30 was proposed by Urry and Mushotzky (1984), who considered a homogeneous source. In particular they applied the constraint derived from the X-ray variability to the dimension of the radio-emitting region. As a consequence, in order to avoid a production of X-rays largely in excess of the observed flux, they were forced to assume that the radiation was relativistically beamed, with a beaming factor

$$\delta = \Gamma(1 - \beta \cos \theta)^{-1} \sim 50 , \qquad (4)$$

where Γ is the Lorentz factor, β is the velocity, θ is the viewing angle. However, the decrease of the variability time scale with increasing energy discussed above strongly suggests an inhomogeneous model of the source, with the inner region being responsible for the X-ray emission and the periphery for the radio. An SSC model of PKS 2155−30 for an inhomogeneous source was proposed by Ghisellini, Maraschi, and Treves (1985), who concluded that there could be no relativistic beaming ($\delta = 1$). This agrees also with the results of Madejski (1985).

c) *Further Theoretical Considerations*

Within the picture given above the X-rays are produced in the inner region of the source, and the minimum time scale of variability of medium-energy X-rays $t_D \approx 2000$ s may be taken as indicative of an upper bound to the dimension of the region of emission, $l < ct_D \sim 6 \times 10^{13}$ cm (see, however on this point, the discussion by Lawrence 1987). As shown in our previous paper (Morini *et al.* 1986), one has that l is less than 2 gravita-

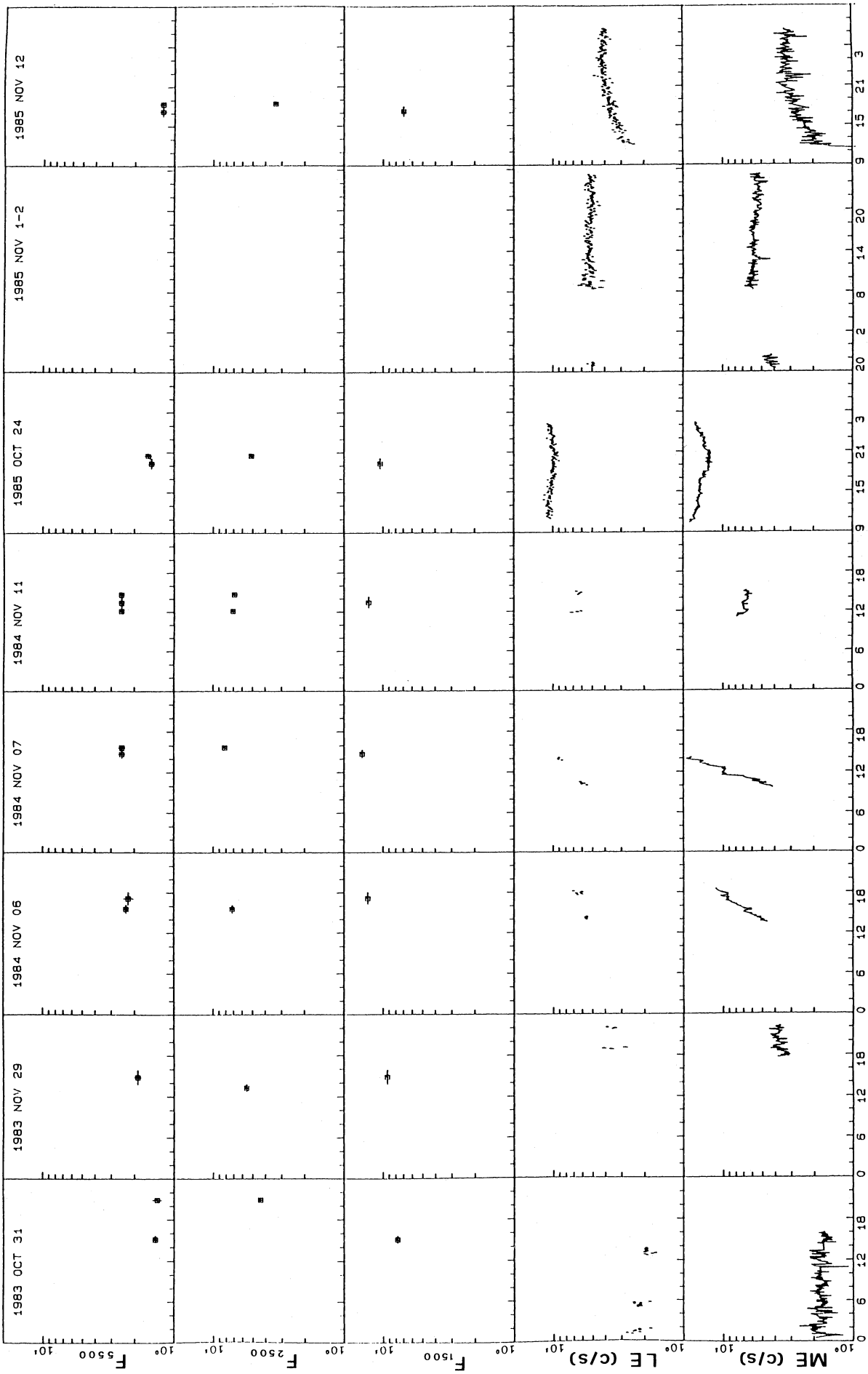

FIG. 9.—Light curve of PKS 2155−304 in different energy bands. From top to bottom: optical flux as from the FES (arbitrary units); flux at 2500 Å and at 1500 Å (arbitrary units); LE count rates in the 3000 Å Lexan filter; ME count rates.

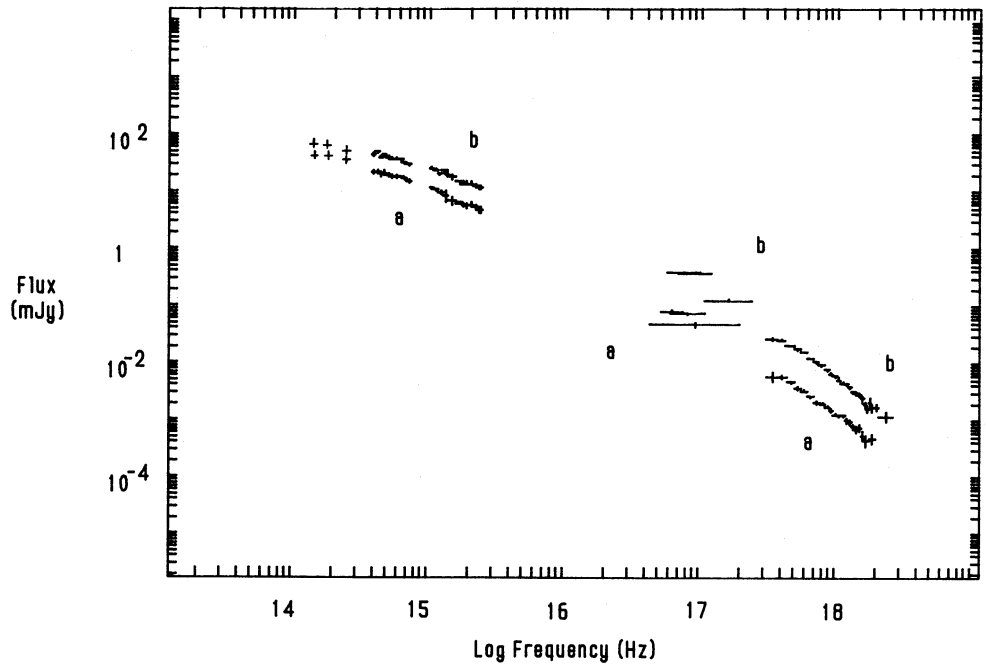

FIG. 10.—Overall energy distribution of PKS 2155−304 for 1983 Oct 30–31 (*lower state*, labeled *a*) and 1984 Nov 11 (*higher state*, labeled *b*). The infrared data at the lower state correspond to observations of 1983 Aug 16, 18.

tional radii, if the total luminosity $\sim 10^{46}$ ergs s^{-1} is supposed to be Eddington-limited (i.e., $M > 10^8 M_\odot$). The constraint is severe and it appears hard to be fulfilled by most models not involving relativistic amplification of the observed radiation. Since the relativistic correction to l scales as $\sim\delta$, the required value of δ could be much lower than that proposed by Urry and Mushotzky (1982).

The X-ray spectrum between ~ 0.1 keV and 10 keV can be described as a power law of energy index $\alpha \approx 1.7$ plus absorption (see above). Because of the brightness of the source the X-ray spectrum is probably the best determined among BL Lac objects. When compared to that of typical Seyfert galaxies and quasars, it appears clearly steeper, at least above ~ 2 keV (see, e.g., Rothschild *et al.* 1983). The steepness of the X-ray spectrum seems to be a characteristic of BL Lac objects as a class (e.g., Urry, Mushotsky, and Holt 1986; Maraschi and Maccagni 1988). The simplest possibility which comes to mind is that the steepness is associated with the steepening of the particles radiating via the synchrotron process, perhaps due to the approach of the maximum injection energy (e.g., Maraschi 1987; Ghisellini and Maraschi 1989). Alternatively, as suggested by White, Fabian, and Mushotzky (1984) on the basis of phenomenological arguments, the steepness of the X-ray spectrum may be a consequence of an emission region, where copious pair production occurs. Since the arguments for producing the radio to optical continuum in BL Lac objects via synchrotron radiation are compelling, pair production should be considered in the framework of SSC models. This was done by Zdziarski (1986) and Ghisellini (1987, 1988). In these models a steep X-ray spectrum can be the result of thermal Comptonization of synchrotron photons, giving rise to a steep tail above the maximal synchrotron frequency. This requires high compactness and a radiation energy density not far from equipartition with the magnetic field. These results, though derived for the case of a homogeneous source, may well be applied to the X-ray emitting region. However an extension of the description to the entire energy distribution should take into account the inhomogeneity of the regions emitting in different frequency bands, clearly revealed by our data.

It seems to us that there is still a large gap between the present observational data and the existing theoretical models. In particular time-dependent models are only now starting to be considered (e.g., Fabian *et al.* 1986). In this respect an important issue for future modeling is the dependence of the spectral shape with intensity. While the intensity (at 2 keV) varied by more than an order of magnitude during our observations, the slope varied only by $\Delta\alpha \approx 0.5$. Taking into account the entire set of data, no correlation between the spectral index and the intensity can be found (see Table 6). However, if one considers separately the episodes of high activity, one finds clearly a hardening of the spectrum with increasing intensity as illustrated by Figure 2, where the ME count rates are plotted versus the LE ones. In X-rays a similar behavior is found during an active state of the BL Lac object Mrk 421 (George, Warwick, and Bromage 1988), where the relevant time scales were of the order of one day.

Because of its brightness and high variability in X-rays, PKS 2155−304 is, in our opinion, a prime candidate for a systematic study on the dynamical evolution of the spectral shape.

We are grateful to G. Ghisellini for a critical reading of the discussion section, and we wish to thank the *IUE* staff at the ESA station at Villafranca (Spain) for competent support. Financial support from Piano Spaziale Nazionale is acknowledged.

REFERENCES

Agrawal, P. C., Singh, K. P., and Riegler, G. R. 1987, *M.N.R.A.S.*, **227**, 525.
Barr, P., Giommi, P., Pollock, A., Tagliaferri, G., Maccagni, D., and Garilli, B. 1988, *EXOSAT* preprint no. 86, to appear in Proc. IAU Symposium N. 134.
Bessel, M. S. 1979, *P.A.S.P.*, **91**, 589.
Bevington, P. R. 1969, *Data Reduction and Error Analysis for the Physical Sciences* (NY: McGraw-Hill).
Bezler, M., Gruber, D. E., and Rothschild, R. E. 1988, *Ap. J.*, **334**, 995.
Bowyer, S., Brodie, J., Clarke, J. T., and Henry, J. P. 1984, *Ap. J. (Letters)*, **278**, L103.
Brown, R. L., and Gould, J. 1970, *Phys. Rev. D*, **1**, 2252.
Canizares, C., and Kruper, J. 1984, *Ap. J. (Letters)*, **278**, L99.
Cooke, B. A., *et al.* 1978, *M.N.R.A.S.*, **182**, 489.
Fabian, A. C., Blanford, R. D., Guibert, P. W., Phinney, E. S., and Cuellar, L. 1986, *M.N.R.A.S.*, **211**, 931.
George, I. M., Warwick, R. S., and Bromage, G. E. 1989, *M.N.R.A.S.*, in press.
Ghisellini, G. 1987, *M.N.R.A.S.*, **224**, 1.
———. 1988, paper presented at the symposium "BL Lac Objects: 10 Years After," Como, 1988 September, in press.
Ghisellini, G., and Maraschi, L. 1989, *Ap. J.*, **340**, 181.
Ghisellini, G., Maraschi, L., and Treves, A. 1985, *Astr. Ap.*, **146**, 204.
Griffiths, R. E., Tapia, S., Briel, U., and Chaisson, L. 1979, *Ap. J.*, **234**, 810.
Guilbert, P. W., Fabian, A. C., and McCray, R. 1983, *Ap. J.*, **266**, 466.
Halpern, J. P. 1984, *Ap. J.*, **281**, 90.
Holm, A., and Crabb, W. G. 1979, *NASA IUE News Letter*, **7**, 40.
Impey, C. D., and Neugebauer, G. 1988, *A.J.*, **95**, 307.
Krolik, J. H., and Kallman, T. R. 1984, *Ap. J.*, **286**, 366.
Krolik, J. H., Kallman, T. R., Fabian, A. C., and Rees, M. J. 1985, *Ap. J.*, **295**, 104.
Lawrence, A. 1987, in *Variability of Galactic and Extragalactic X-Ray Sources*, ed. A. Treves, Associazione Avanzamento Astronomia, Milano-Bologna, p. 29.
Madejski, G. 1985, Ph.D. thesis, Harvard University.
Maraschi, L. 1987, in *Variability of Galactic and Extragalactic X-Ray Sources*, ed. A. Treves, Associazione Avanzamento Astronomia, Milano-Bologna.
Maraschi, L., and Maccagni, D. 1988, "X-ray Astronomy with EXOSAT," ed. R. Pallavicini and N. White (*Mem. Soc. Astr. Italiana*, **59**, 277).
Maraschi, L., Tagliaferri, G., Tanzi, E. G., and Treves, A. 1986, *Ap. J.*, **304**, 637.
Miller, H. R., and McAlister, H. A. 1983, *Ap. J.*, **272**, 26.
Miyoshi, S., Hayakawa, S., Kunieda, H., Nagase, F., and Tawara, Y. 1986, *Ap. Space Sci.*, **119**, 185.
Morini, M., *et al.* 1986, *Ap. J. (Letters)*, **306**, L71.
Morini, M., Chiappetti, L., Maraschi, L., Tagliaferri, G., Tanzi, E. G., and Treves, A. 1987, in *Variability of Galactic and Extragalactic X-ray Sources*, ed. A. Treves, (Milano Bologna: Associazione Avanzamento Astronomia).
Morini, M., Lipani, N. A., and Molteni, D. 1987, *Ap. J.*, **317**, 145.
Rothschild, R. E., Mushotsky, R. F., Baity, W. A., Gruber, D. E., Matteson, J. L., and Peterson, L. E. 1983, *Ap. J.*, **269**, 423.
Schwartz, D. A., Doxsey, R. E., Griffiths, R. E., Johnston, M. D., and Schwarz, J. 1979, *Ap. J. (Letters)*, **229**, L53.
Simpson, G., and Mayer Hasselwander, H. 1986, *Astr. Ap.*, **162**, 340.
Snyder, W. A., *et al.* 1980, *Ap. J. (Letters)*, **237**, L11.
Stark, A. A., Heiles, C., Bally, J., and Linke, R. 1988, in preparation.
Tagliaferri, G., Stella, L., Maraschi, L., Treves, A., and Morini, M. 1988, paper presented at the symposium "BL Lac Objects: 10 Years After," Como, 1988 September, in press.
Tanzi, E. G., *et al.* 1984, in *Fourth European IUE Conference* (*ESA SP 218*), p. 111.
Taylor, B. G., Andresen, R. D., Peacock, A., and Zobl, R. 1981, *Space Sci. Rev.*, **30**, 479.
Ulvestad, J. S., and Antonucci, R. R. J. 1986, *A.J.*, **92**, 6.
Urry, C. M., and Mushotzky, R. F. 1982, *Ap. J.*, **253**, 38.
Urry, C. M., Kondo, Y., Hackney, K. R. H., and Hackney, R. L. 1988, *Ap. J.*, **330**, 791.
Urry, C. M., Mushotzky, R. F., and Holt, S. S. 1986, *Ap. J.*, **305**, 369.
White, N. E., Fabian, A. C., and Mushotzky, R. F. 1984, *Astr. Ap.*, **133**, L9.
Zdziarski, A. 1986, *Ap. J.*, **305**, 45.

L. CHIAPPETTI, D. MACCAGNI, and E. G. TANZI: Istituto di Fisica Cosmica del C.N.R., Via Bassini 15, 20133, Milano, Italy

A. FABIAN: Institute of Astronomy, Madingley Road, Cambridge, CB3 0HA, England

R. FALOMO: Osservatorio Astronomico, Vicolo dell'Osservatorio 5, 35100 Padova, Italy

L. MARASCHI and A. TREVES: Dipartimento di Fisica dell'Università, Via Celoria 16, 20133 Milano, Italy

M. MORINI: Istituto di Fisica Cosmica ed Applicazioni all'Informatica del C.N.R., Via M. Stabile 172, 90139 Palermo, Italy

G. TAGLIAFERRI: ESTEC, Postbus 299, 2200 AG Noordwijk, The Netherlands